Radiat Environ Biophys (2011) 50:441–450
DOI 10.1007/s00411-011-0370-0

ORIGINAL PAPER

Assessment of MIRD data for internal dosimetry using the GATE Monte Carlo code

Ali Asghar Parach · Hossein Rajabi · Mohammad Ali Askari

Received: 31 January 2011 / Accepted: 1 May 2011 / Published online: 15 May 2011

Abstract GATE/GEANT is a Monte Carlo code dedicated to nuclear medicine that allows calculation of the dose to organs of voxel phantoms. On the other hand, MIRD is a well-developed system for estimation of the dose to human organs. In this study, results obtained from GATE/GEANT using Snyder phantom are compared to published MIRD data. For this, the mathematical Snyder phantom was discretized and converted to a digital phantom of 100 × 200 × 360 voxels. The activity was considered uniformly distributed within kidneys, liver, lungs, pancreas, spleen, and adrenals. The GATE/GEANT Monte Carlo code was used to calculate the dose to the organs of the phantom from mono-energetic photons of 10, 15, 20, 30, 50, 100, 200, 500, and 1000 keV. The dose was converted into specific absorbed fraction (SAF) and the results were compared to the corresponding published MIRD data. On average, there was a good correlation (r^2>0.99) between the two series of data. However, the GATE/GEANT data were on average −0.16 ± 6.22% lower than the corresponding MIRD data for self-absorption. Self-absorption in the lungs was considerably higher in the MIRD compared to the GATE/GEANT data, for photon energies of 10–20 keV. As for cross-irradiation to other organs, the GATE/GEANT data were on average +1.5 ± 8.1% higher than the MIRD data, for photon energies of 50–1000 keV. For photon energies of 10–30 keV, the relative difference was +7.5 ± 67%. It turned out that the agreement between the GATE/GEANT and the MIRD data depended upon absolute SAF values and photon energy. For 10–30 keV photons, where the absolute SAF values were small, the uncertainty was high and the effect of cross-section prominent, and there was no agreement between the GATE/GEANT results and the MIRD data. However, for photons of 50–1,000 keV, the bias was negligible and the agreement was acceptable.

A. A. Parach · H. Rajabi (✉) · M. A. Askari
Department of Medical Physics, Faculty of Medical Sciences, Tarbiat Modares University, P.O. Box 14115-331 Tehran, Iran
e-mail: hRajabi@modares.ac.ir

Introduction

Radioisotopes are used in nuclear medicine in a variety of diagnostic and therapeutic procedures. In most applications, a significant absorbed dose may be received by some radiosensitive organs (Stabin 2003). This requires dose quantification, to balance between the risks and the benefits in any application involving the use of radioisotopes in humans. Unfortunately, direct measurement of the absorbed dose in organs of the human body from administrated radioisotopes is not possible. Therefore, internal dose assessment is often performed using pre-calculated reference data derived from humanoid anatomical models. For many years, the Medical Internal Radiation Dose (MIRD) committee of the American society of nuclear medicine has been the main source of reference data for dose assessment in nuclear medicine (Chao and Xu 2004; Ferrari and Gualdrini 2007; Wessels et al. 2006).

MIRD and its subsequent developments (Bouchet et al. 2003, 1999; Howell et al. 1999; Siegel et al. 1999; Snyder et al. 1975; Stabin 1996; Stabin et al. 2005) have been useful for estimation of the organ dose in diagnostic and protection objectives. However, because of some limitations, their application in therapeutic procedures is limited (Kolbert et al. 1997; Lyra and Phinou 2000). For example, the MIRD reference data are calculated assuming a uniform distribution of radioisotopes in the organs of a limited number of humanoid models. Furthermore, therapeutic

application of radioisotopes generally involves estimation of dose to the tumors. Although a simple form of tumor is considered in OLINDA (Stabin et al. 2005), which is the software implementing the MIRD data, it is almost impossible to consider all types of tumors in the MIRD humanoid models. These limitations make it necessary to calculate the dose on an individual basis, in therapeutic applications (Dewaraja et al. 2005; Kolbert et al. 1997).

Monte Carlo simulations using computational phantoms are a powerful tool and have therefore been widely used in dosimetry calculations (Williams 2003; Yoriyaz et al. 2001; Franquiz et al. 2003; Furhang et al. 1997, 1996; Taschereau and Chatziioannou 2007; Visvikis et al. 2006; Saito et al. 2001). Today, mathematical, voxelized, and hybrid computational phantoms are being used with Monte Carlo techniques, to calculate absorbed doses to human organs and tissues irradiated with ionizing radiation involving internal radioactive sources (Bolch et al. 2010; Caon 2004). Monte Carlo simulation can be considered as the most suitable method for patient-specific dosimetry (Akabani et al. 1997; Dewaraja et al. 2005; Sgouros et al. 2004). The physical properties of the tissues involved and the distribution of radioisotopes can be determined using CT and SPECT (or PET) images. There are many Monte Carlo codes available that can be used to estimate radiation dose within the body at the organ or pixel level (Chiavassa et al. 2005; Furhang et al. 1997; Ljungberg et al. 2002; Sgouros et al. 2004; Stabin 2008).

GATE (Geant4 Application for Tomographic Emission), a code dedicated for nuclear medicine application, has recently been developed as the upper layer of the GEANT4 toolkit (Santin et al. 2007). GATE/GEANT has been developed with the ambition to become the gold standard in nuclear medicine. It has a great potential to be used for individual dosimetry. The data derived from many Monte Carlo codes have already been compared to the MIRD data for different purposes (Ferrari and Gualdrini 2007; Hadid et al. 2010; Smith et al. 2000; Zankl et al. 2003). There have already been some efforts to also validate GATE/GEANT data for internal dosimetry applications (Ludovic et al. 2007; Taschereau and Chatziioannou 2005, 2007; Thiam et al. 2008; Visvikis et al. 2006). However, MIRD data have never been compared to the data derived from GATE/GEANT. Such comparison is important because GATE/GEANT is the only open access Monte Carlo code dedicated for nuclear medicine that allows calculation of a dose map within the patients' body. On the other hand, MIRD is the most developed system for internal dose assessment in nuclear medicine.

In the present study, the digital form of the Snyder mathematical phantom was constructed and used with GATE/GEANT to calculate the dose to the organs of the phantom. The results were compared to the previously published MIRD data (Snyder et al. 1969).

Materials and methods

Phantom

To construct a voxel phantom identical to the phantom used in the MIRD calculations, the mathematical equations (Snyder et al. 1969) used to describe the organs of the phantom were converted into discrete forms. The Snyder mathematical phantom was sampled at a spatial resolution of $2 \times 2 \times 3$ mm and converted to a voxel phantom of $100 \times 200 \times 360$ matrix size (from head to mid-thigh). The digitalization was optimized to minimize the sum of differences between the volumes of the organs in the digital and mathematical phantoms (Press et al. 2007). Because the simulation of each source organ should be performed separately, six copies of the digital phantom were generated; one phantom for each organ, and the activity of interest was distributed uniformly within the kidneys, liver, lungs, pancreas, spleen, and the adrenal glands of the phantoms, respectively.

Monte Carlo simulation

The GATE/GEANT Monte Carlo package (version 4.0.0) was used to calculate the dose to the organs of the phantoms (Jan et al. 2004; Santin et al. 2007; Visvikis et al. 2006). Each voxel in the phantoms was linked to a table describing the attenuation properties (composition and density) of the corresponding tissue. The table was constructed based on the data described in the MIRD publications (Snyder et al. 1969). Simulations were performed (each phantom separately) for photons of 10, 15, 20, 30, 50, 100, 200, 500, and 1,000 keV. In each simulation, 2×10^8 photons were tracked. The simulation time was between 3 and 10 h. Compton scattering, photoelectric absorption, and Rayleigh scattering were considered in the photon tracking. Scattered photons were tracked down to 1 keV. At the end of each simulation, a file containing the dose deposited per voxel of the phantom was created. No variance reduction technique was used in the simulations.

Calculation of SAF values

In the MIRD formalism, the reference data are presented in terms of specific absorbed fraction (SAF) values (Blaickner and Kindl 2008; Smith et al. 2000; Snyder et al. 1969). SAF is a net factor that converts the total energy emitted from a particular source organ to the energy absorbed in another organs (cross-irradiation) or the same organ itself

(self-absorption) (Sgouros 2005). SAF is defined for each pair of source organ (r_s) and target organ (r_t) as follows:

$$\mathrm{SAF}(r_t \xleftarrow{E} r_s) = \frac{\text{energy absorbed in } r_t / \text{energy emitted from } r_s}{m}. \quad (1)$$

where m is the mass of the target organ in kilogram (kg). The absorbed energy in each organ was calculated as sum of the absorbed energy in the entire voxels of the organ. For calculation of organ masses, the total number of voxels belonging to an organ was determined and then multiplied by voxel volume and the density of corresponding organ using MIRD data (Snyder et al. 1969).

Data analysis

The relative difference (RD) between SAF values derived from GATE/GEANT ($\mathrm{SAF_{GATE}}$) and the corresponding MIRD values ($\mathrm{SAF_{MIRD}}$) for each photon energy was calculated as

$$\mathrm{RD}\% = 100 \times \left(\frac{\mathrm{SAF_{GATE}} - \mathrm{SAF_{MIRD}}}{\mathrm{SAF_{MIRD}}}\right). \quad (2)$$

GATE/GEANT and the corresponding MIRD data were compared through fitting a linear curve to the scatter plot of the data and calculating the Pearson's correlation coefficient. Also, a Bland–Altman plot was used to determine the agreement and bias between the GATE/GEANT results and the MIRD data (Bland and Altman 2010). Analyses were performed independently for the self-absorption and cross-irradiation data.

Results

The volumes of the organs in the mathematical Snyder phantom and in its digital form are presented in Table 1. The maximum relative difference between the volumes of the corresponding organs in the two phantoms was 2.7% (sigmoid colon) and the minimum difference was 0.08% (liver). For the organs considered in the present study, the maximum relative difference was 0.4%.

SAFs obtained for liver, kidneys, lungs, pancreas, spleen, and adrenal glands (as source organs) are presented in Tables 2, 3, 4, 5, 6, and 7, respectively. The MIRD SAF values were also included in the tables for the sake of comparison (Snyder et al. 1969).

SAFs for the self-absorption

Figure 1a shows the scatter plot and the linear curve fitted to the MIRD and GATE/GEANT data for photons of 10–1,000 keV. Due to the wide range of SAF values, the graph is shown in logarithmic scale. The figure clearly shows a good linear correlation ($r = 0.999$) between the two series of data. However, the slope of the curve is slightly below unity (+0.994) and the intercept is slightly above zero (+0.009). This implies a little bias between the MIRD and the GATE/GEANT data, for the self-absorption in the organs considered in the present study. The Bland–Altman plot (Fig. 1b) reveals that the SAF values derived from GATE/GEANT are on average 0.16% smaller than the corresponding MIRD values. As Fig. 1b shows, most of the data points are within two standard deviations from the mean (i.e., within $-0.16 \pm 6.22\%$ including the lungs). However, the data points derived for lungs had a distinct different distribution from the rest of the data points (marked in Fig. 1b). The relative differences (%RD) for these data points were noticeably higher, positive, and inversely proportional to the photon energy.

Table 1 Volumes of the organs in the mathematical and voxelized Snyder phantom

Organ	Organ volume (cm3)		
	Snyder phantom	Voxel snyder phantom	%RD[a]
Adrenals	15.71	15.65	0.38
Brain	1470	1504	2.31
Clavicles	54.7	53.6	2.01
Heart	603.1	601.7	0.23
Kidneys	288	288.7	0.24
Liver	1833	1831.5	0.08
Lower large intestine	101.63	100.6	1.01
Lungs	3378	3376.6	0.04
Ovaries	8.38	8.35	0.36
Pancreas	61.07	61.32	0.41
Pelvis	606.1	597.6	1.40
Rib cages	694	691	0.43
Scapula	201.4	200	0.70
Sigmoid colon	35.63	36.59	2.69
Skull	846.6	839.3	0.86
Small intestine	1054	1042.2	1.12
Spine	887.5	893.9	0.72
Spleen	175.9	175.44	0.26
Stomach	250.2	249.9	0.12
Testicles	37.57	37.5	0.19
Thyroid	19.89	20.33	2.21
Transverse colon	126.7	126	0.55
Upper large intestine	96.29	94.49	1.87
Urinary bladder	202.6	201.2	0.69
Uterus	66.27	66.16	0.17

[a] Relative difference

Table 2 SAF values in Snyder phantom (kg^{-1}) for liver as source

		Photon energy (keV)								
Target	Method	10	15	20	30	50	100	200	500	1,000
Liver	GATE	5.36E-01	4.98E-01	4.35E-01	2.96E-01	1.51E-01	9.02E-02	8.67E-02	8.72E-02	7.96E-02
	MIRD	5.36E-01	4.96E-01	4.34E-01	2.97E-01	1.52E-01	9.14E-02	8.82E-02	8.85E-02	8.07E-02
	%RD	0.00E+00	4.03E-01	2.30E-01	3.37E-01	6.58E-01	1.31E+00	1.70E+00	1.47E+00	1.36E+00
Kidneys	GATE	1.01E-05	7.11E-04	4.35E-03	1.56E-02	1.94E-02	1.51E-02	1.37E-02	1.32E-02	1.23E-02
	MIRD	8.30E-04	1.26E-03	4.50E-03	1.57E-02	1.95E-02	1.58E-02	1.36E-02	1.29E-02	1.18E-02
	%RD	9.88E+01	4.36E+01	3.33E+00	6.37E-01	5.13E-01	4.43E+00	7.35E-01	2.33E+00	4.24E+00
Lungs	GATE	3.85E-04	4.36E-03	1.07E-02	1.71E-02	1.47E-02	1.01E-02	8.98E-03	8.67E-03	8.01E-03
	MIRD	8.00E-05	3.19E-03	9.46E-03	1.64E-02	1.45E-02	9.90E-03	8.84E-03	8.20E-03	7.90E-03
	%RD	3.81E+02	3.67E+01	1.31E+01	4.27E+00	1.38E+00	2.02E+00	1.58E+00	5.73E+00	1.39E+00
Pancreas	GATE	1.66E-07	2.28E-04	3.64E-03	1.77E-02	2.32E-02	1.81E-02	1.58E-02	1.47E-02	1.34E-02
	MIRD	1.47E-03	2.21E-03	2.94E-03	1.67E-02	2.18E-02	1.77E-02	1.35E-02	1.66E-02	1.36E-02
	%RD	1.00E+02	8.97E+01	2.38E+01	5.99E+00	6.42E+00	2.26E+00	1.70E+01	1.14E+01	1.47E+00
Spleen	GATE	0.00E+00	0.00E+00	8.25E-06	7.09E-04	3.17E-03	3.87E-03	3.72E-03	3.71E-03	3.66E-03
	MIRD	7.27E-10	1.09E-09	4.57E-06	1.64E-03	2.93E-03	3.56E-03	3.34E-03	3.44E-03	3.80E-03
	%RD	1.00E+02	1.00E+02	8.05E+01	5.68E+01	8.19E+00	8.71E+00	1.14E+01	7.85E+00	3.68E+00
Adrenals	GATE	3.83E-04	4.51E-03	1.41E-02	2.67E-02	2.54E-02	1.88E-02	1.73E-02	1.66E-02	1.56E-02
	MIRD	2.45E-03	3.68E-03	1.36E-02	2.68E-02	2.15E-02	1.61E-02	1.81E-02	1.68E-02	1.56E-02
	%RD	8.44E+01	2.26E+01	3.68E+00	3.73E-01	1.81E+01	1.68E+01	4.42E+00	1.19E+00	0.00E+00

Table 3 SAF values in Snyder phantom (kg^{-1}) for kidneys as source

		Photon energy (keV)								
Target	Method	10	15	20	30	50	100	200	500	1,000
Liver	GATE	1.02E-05	7.07E-04	4.37E-03	1.57E-02	1.96E-02	1.53E-02	1.38E-02	1.32E-02	1.23E-02
	MIRD	4.40E-04	6.65E-04	4.68E-03	1.54E-02	1.95E-02	1.53E-02	1.36E-02	1.38E-02	1.22E-02
	%RD	9.77E+01	6.32E+00	6.62E+00	1.95E+00	5.13E-01	0.00E+00	1.47E+00	4.35E+00	8.20E-01
Kidneys	GATE	3.26E+00	2.74E+00	2.04E+00	1.02E+00	3.91E-01	2.27E-01	2.35E-01	2.45E-01	2.22E-01
	MIRD	3.28E+00	2.74E+00	2.04E+00	1.03E+00	3.93E-01	2.35E-01	2.39E-01	2.52E-01	2.26E-01
	%RD	6.10E-01	0.00E+00	0.00E+00	9.71E-01	5.09E-01	3.40E+00	1.67E+00	2.78E+00	1.77E+00
Lungs	GATE	0.00E+00	3.34E-07	7.43E-05	1.54E-03	3.60E-03	3.60E-03	3.44E-03	3.53E-03	3.47E-03
	MIRD	3.57E-05	5.36E-05	7.15E-05	1.18E-03	3.27E-03	3.37E-03	2.99E-03	3.28E-03	3.30E-03
	%RD	1.00E+02	9.94E+01	3.92E+00	3.05E+01	1.01E+01	6.82E+00	1.51E+01	7.62E+00	5.15E+00
Pancreas	GATE	0.00E+00	5.22E-05	3.55E-03	2.60E-02	3.45E-02	2.65E-02	2.33E-02	2.18E-02	1.99E-02
	MIRD	2.34E-05	3.51E-05	4.45E-03	2.44E-02	3.22E-02	2.63E-02	2.28E-02	2.25E-02	2.24E-02
	%RD	1.00E+02	4.87E+01	2.02E+01	6.56E+00	7.14E+00	7.60E-01	2.19E+00	3.11E+00	1.12E+01
Spleen	GATE	1.46E-04	8.67E-03	3.63E-02	6.77E-02	5.18E-02	3.33E-02	3.04E-02	2.96E-02	2.73E-02
	MIRD	6.19E-03	9.28E-03	3.63E-02	6.69E-02	5.32E-02	3.30E-02	3.11E-02	2.85E-02	2.70E-02
	%RD	9.76E+01	6.57E+00	0.00E+00	1.20E+00	2.63E+00	9.09E-01	2.25E+00	3.86E+00	1.11E+00
Adrenals	GATE	5.62E-03	3.70E-02	7.59E-02	9.28E-02	6.18E-02	4.04E-02	3.85E-02	3.85E-02	3.56E-02
	MIRD	4.70E-03	3.95E-02	8.11E-02	9.44E-02	6.30E-02	4.51E-02	3.48E-02	4.28E-02	4.01E-02
	%RD	1.96E+01	6.33E+00	6.41E+00	1.69E+00	1.90E+00	1.04E+01	1.06E+01	1.00E+01	1.12E+01

SAFs for cross-irradiation

The results of a similar analysis for the cross-irradiation data are presented in Fig. 2a, b. The curve fitted to the scatter plot of the data (Fig. 2a) shows a good linear correlation between the SAF values derived from GATE/GEANT and the corresponding MIRD data. However, visual inspection of Fig. 2a reveals that the correlation

Table 4 SAF values in Snyder phantom (kg^{-1}) for lungs as source

		Photon energy (keV)								
Target	Method	10	15	20	30	50	100	200	500	1,000
Liver	GATE	3.44E-04	3.88E-03	9.54E-03	1.54E-02	1.35E-02	9.71E-03	8.91E-03	8.67E-03	8.04E-03
	MIRD	7.00E-05	2.28E-03	7.25E-03	1.40E-02	1.29E-02	9.50E-03	8.81E-03	8.20E-03	7.70E-03
	%RD	3.91E+02	7.02E+01	3.16E+01	1.00E+01	4.65E+00	2.21E+00	1.14E+00	5.73E+00	4.42E+00
Kidneys	GATE	0.00E+00	2.10E-07	6.90E-05	1.40E-03	3.28E-03	3.43E-03	3.38E-03	3.53E-03	3.47E-03
	MIRD	6.42E-08	9.64E-08	5.81E-05	1.24E-03	2.97E-03	3.25E-03	3.14E-03	3.61E-03	3.22E-03
	%RD	1.00E+02	1.18E+02	1.88E+01	1.29E+01	1.04E+01	5.54E+00	7.64E+00	2.22E+00	7.76E+00
Lungs	GATE	9.12E-01	7.29E-01	5.10E-01	2.41E-01	9.25E-02	5.11E-02	5.04E-02	5.09E-02	4.50E-02
	MIRD	8.17E-01	6.58E-01	4.71E-01	2.30E-01	8.99E-02	5.05E-02	5.00E-02	5.01E-02	4.55E-02
	%RD	1.16E+01	1.08E+01	8.28E+00	4.78E+00	2.89E+00	1.19E+00	8.00E-01	1.60E+00	1.10E+00
Pancreas	GATE	0.00E+00	2.10E-05	1.20E-03	8.75E-03	1.23E-02	9.96E-03	8.92E-03	8.42E-03	7.73E-03
	MIRD	8.53E-06	1.28E-05	6.38E-04	9.00E-03	1.27E-02	1.04E-02	8.94E-03	9.63E-03	7.11E-03
	%RD	1.00E+02	6.41E+01	8.81E+01	2.78E+00	3.15E+00	4.23E+00	2.24E-01	1.26E+01	8.72E+00
Spleen	GATE	3.70E-05	1.26E-03	5.50E-03	1.27E-02	1.23E-02	9.00E-03	8.22E-03	7.98E-03	7.45E-03
	MIRD	6.63E-04	9.95E-04	4.70E-03	1.27E-02	1.10E-02	9.00E-03	8.18E-03	7.10E-03	7.20E-03
	%RD	9.44E+01	2.66E+01	1.70E+01	0.00E+00	1.18E+01	0.00E+00	4.89E-01	1.24E+01	3.47E+00
Adrenals	GATE	6.40E-07	7.18E-04	5.21E-03	1.43E-02	1.39E-02	1.08E-02	1.01E-02	9.76E-03	9.36E-03
	MIRD	1.24E-03	1.86E-03	2.48E-03	7.17E-03	1.13E-02	1.09E-02	8.77E-03	8.40E-03	7.73E-03
	%RD	9.99E+01	6.14E+01	1.10E+02	9.94E+01	2.30E+01	9.17E-01	1.52E+01	1.62E+01	2.11E+01

Table 5 SAF values in Snyder phantom (kg^{-1}) for pancreas as source

		Photon energy (keV)								
Target	Method	10	15	20	30	50	100	200	500	1,000
Liver	GATE	1.38E-07	2.33E-04	3.66E-03	1.77E-02	2.32E-02	1.79E-02	1.57E-02	1.46E-02	1.34E-02
	MIRD	1.54E-04	2.30E-04	3.61E-03	1.64E-02	2.24E-02	1.76E-02	1.56E-02	1.41E-02	1.29E-02
	%RD	9.99E+01	1.30E+00	1.39E+00	7.93E+00	3.57E+00	1.70E+00	6.41E-01	3.55E+00	3.88E+00
Kidneys	GATE	0.00E+00	5.18E-05	3.56E-03	2.59E-02	3.41E-02	2.60E-02	2.31E-02	2.16E-02	1.98E-02
	MIRD	2.00E-05	3.39E-05	3.23E-03	2.50E-02	3.37E-02	2.65E-02	2.27E-02	2.13E-02	1.94E-02
	%RD	1.00E+02	5.28E+01	1.02E+01	3.60E+00	1.19E+00	1.89E+00	1.76E+00	1.41E+00	2.06E+00
Lungs	GATE	0.00E+00	2.48E-05	1.34E-03	9.60E-03	1.34E-02	1.03E-02	8.95E-03	8.39E-03	7.71E-03
	MIRD	2.75E-06	4.12E-06	1.16E-03	8.87E-03	1.29E-02	1.02E-02	8.92E-03	8.21E-03	7.43E-03
	%RD	1.00E+02	5.02E+02	1.55E+01	8.23E+00	3.88E+00	9.80E-01	3.36E-01	2.19E+00	3.77E+00
Pancreas	GATE	1.46E+01	1.09E+01	7.18E+00	3.12E+00	1.10E+00	6.32E-01	6.68E-01	7.03E-01	6.25E-01
	MIRD	1.47E+01	1.09E+01	7.14E+00	3.16E+00	1.10E+00	6.51E-01	6.88E-01	7.29E-01	6.74E-01
	%RD	6.80E-01	0.00E+00	5.60E-01	1.27E+00	0.00E+00	2.92E+00	2.91E+00	3.57E+00	7.27E+00
Spleen	GATE	1.79E-03	4.34E-02	1.26E-01	1.78E-01	1.20E-01	7.33E-02	6.61E-02	6.38E-02	5.84E-02
	MIRD	1.45E-06	4.48E-02	1.31E-01	1.79E-01	1.25E-01	7.62E-02	6.70E-02	6.59E-02	5.78E-02
	%RD	1.23E+05	3.13E+00	3.82E+00	5.59E-01	4.00E+00	3.81E+00	1.34E+00	3.19E+00	1.04E+00
Adrenals	GATE	0.00E+00	6.30E-05	5.99E-03	3.90E-02	4.62E-02	3.45E-02	3.10E-02	2.90E-02	2.63E-02
	MIRD	3.02E-05	4.54E-05	4.82E-03	3.96E-02	4.60E-02	3.80E-02	2.95E-02	2.90E-02	2.10E-02
	%RD	1.00E+02	3.88E+01	2.43E+01	1.52E+00	4.35E-01	9.21E+00	5.08E+00	0.00E+00	2.52E+01

between the two series of data depends on the absolute values of the SAF, so that the correlation decreases as the absolute value of the SAF decreases. The Bland–Altman plot (Fig. 2b) clearly shows that the data points follow two different distributions. Calculations showed that, where the absolute values of the SAFs were above 0.01, the average and standard deviation of the relative differences (%RD) are $+1.5 \pm 8.1\%$. In contrast, where the absolute values of

Table 6 SAF values in Snyder phantom (kg^{-1}) for spleen as source

		Photon energy (keV)								
Target	Method	10	15	20	30	50	100	200	500	1000
Liver	GATE	0.00E+00	0.00E+00	7.78E-06	7.02E-04	3.14E-03	3.90E-03	3.72E-03	3.72E-03	3.66E-03
	MIRD	7.20E-10	1.08E-09	4.25E-06	5.99E-04	2.93E-03	3.78E-03	3.67E-03	3.69E-03	3.53E-03
	%RD	1.00E+02	1.00E+02	8.31E+01	1.72E+01	7.17E+00	3.17E+00	1.36E+00	8.13E-01	3.68E+00
Kidneys	GATE	1.43E-04	8.65E-03	3.62E-02	6.77E-02	5.15E-02	3.31E-02	3.03E-02	2.95E-02	2.74E-02
	MIRD	7.02E-03	1.05E-02	3.63E-02	6.65E-02	5.30E-02	3.61E-02	3.14E-02	2.93E-02	2.59E-02
	%RD	9.80E+01	1.76E+01	2.75E-01	1.80E+00	2.83E+00	8.31E+00	3.50E+00	6.83E-01	5.79E+00
Lungs	GATE	3.98E-05	1.41E-03	6.12E-03	1.42E-02	1.34E-02	9.31E-03	8.31E-03	8.03E-03	7.43E-03
	MIRD	6.50E-04	9.76E-04	4.97E-03	1.25E-02	1.23E-02	8.90E-03	7.91E-03	7.50E-03	6.87E-03
	%RD	9.39E+01	4.45E+01	2.31E+01	1.36E+01	8.94E+00	4.61E+00	5.06E+00	7.07E+00	8.15E+00
Pancreas	GATE	1.81E-03	4.35E-02	1.26E-01	1.78E-01	1.21E-01	7.35E-02	6.63E-02	6.39E-02	5.83E-02
	MIRD	1.56E-03	4.29E-02	1.26E-01	1.87E-01	1.23E-01	7.35E-02	6.58E-02	6.70E-02	5.80E-02
	%RD	1.60E+01	1.40E+00	0.00E+00	4.81E+00	1.63E+00	0.00E+00	7.60E-01	4.63E+00	5.17E-01
Spleen	GATE	5.43E+00	4.69E+00	3.59E+00	1.87E+00	7.27E-01	4.13E-01	4.23E-01	4.40E-01	3.98E-01
	MIRD	5.44E+00	4.66E+00	3.59E+00	1.86E+00	7.24E-01	4.21E-01	4.32E-01	4.49E-01	4.10E-01
	%RD	1.84E-01	6.44E-01	0.00E+00	5.38E-01	4.14E-01	1.90E+00	2.08E+00	2.00E+00	2.93E+00
Adrenals	GATE	0.00E+00	2.45E-04	7.08E-03	3.29E-02	3.47E-02	2.45E-02	2.24E-02	2.16E-02	2.02E-02
	MIRD	1.11E-04	1.66E-04	9.76E-03	3.35E-02	3.43E-02	2.40E-02	2.32E-02	2.07E-02	2.35E-02
	%RD	1.00E+02	4.76E+01	2.75E+01	1.79E+00	1.17E+00	2.08E+00	3.45E+00	4.35E+00	1.40E+01

Table 7 SAF values in Snyder phantom (kg^{-1}) for adrenals as source

		Photon energy (keV)								
Target	Method	10	15	20	30	50	100	200	500	1000
Liver	GATE	3.39E-04	4.44E-03	1.40E-02	2.67E-02	2.56E-02	1.93E-02	1.75E-02	1.69E-02	1.69E-02
	MIRD	2.70E-04	4.14E-03	1.28E-02	2.64E-02	2.55E-02	1.93E-02	1.76E-02	1.68E-02	1.50E-02
	%RD	2.56E+01	7.25E+00	9.38E+00	1.14E+00	3.92E-01	0.00E+00	5.68E-01	5.95E-01	1.27E+01
Kidneys	GATE	5.59E-03	3.68E-02	7.63E-02	9.33E-02	6.16E-02	4.10E-02	3.87E-02	3.86E-02	3.86E-02
	MIRD	4.20E-03	3.71E-02	7.53E-02	9.37E-02	5.90E-02	4.25E-02	4.12E-02	3.95E-02	3.59E-02
	%RD	3.31E+01	8.09E-01	1.33E+00	4.27E-01	4.41E+00	3.53E+00	6.07E+00	2.28E+00	7.52E+00
Lungs	GATE	2.31E-06	7.67E-04	5.80E-03	1.59E-02	1.55E-02	1.14E-02	1.03E-02	9.95E-03	9.95E-03
	MIRD	3.19E-04	4.79E-04	3.07E-03	1.03E-02	1.20E-02	9.50E-03	8.91E-03	7.90E-03	7.72E-03
	%RD	9.93E+01	6.01E+01	8.89E+01	5.44E+01	2.92E+01	2.00E+01	1.56E+01	2.59E+01	2.89E+01
Pancreas	GATE	0.00E+00	7.29E-05	5.96E-03	3.94E-02	4.73E-02	3.55E-02	3.13E-02	2.92E-02	2.92E-02
	MIRD	3.02E-05	4.54E-05	7.51E-03	3.84E-02	4.70E-02	3.60E-02	3.03E-02	2.90E-02	2.80E-02
	%RD	1.00E+02	6.06E+01	2.06E+01	2.60E+00	6.38E-01	1.39E+00	3.30E+00	6.90E-01	4.29E+00
Spleen	GATE	0.00E+00	2.36E-04	7.07E-03	3.32E-02	3.51E-02	2.50E-02	2.25E-02	2.16E-02	2.16E-02
	MIRD	4.17E-04	6.26E-04	7.29E-03	3.22E-02	3.48E-02	2.41E-02	2.37E-02	2.22E-02	1.95E-02
	%RD	1.00E+02	6.23E+01	3.02E+00	3.11E+00	8.62E-01	3.73E+00	5.06E+00	2.70E+00	1.08E+01
Adrenals	GATE	5.17E+01	3.29E+01	1.89E+01	7.02E+00	2.21E+00	1.31E+00	1.43E+00	1.53E+00	1.53E+00
	MIRD	5.22E+01	3.29E+01	1.89E+01	7.04E+00	2.23E+00	1.33E+00	1.45E+00	1.57E+00	1.51E+00
	%RD	9.58E-01	0.00E+00	0.00E+00	2.84E-01	8.97E-01	1.50E+00	1.38E+00	2.55E+00	1.32E+00

the SAFs were below 0.01, the average and standard deviation of the relative differences (%RD) are $+7.5 \pm 67.1\%$.

In Fig. 3a, the average relative differences between the MIRD and the GATE/GEANT data are plotted independently against the photon energies for the self-absorption

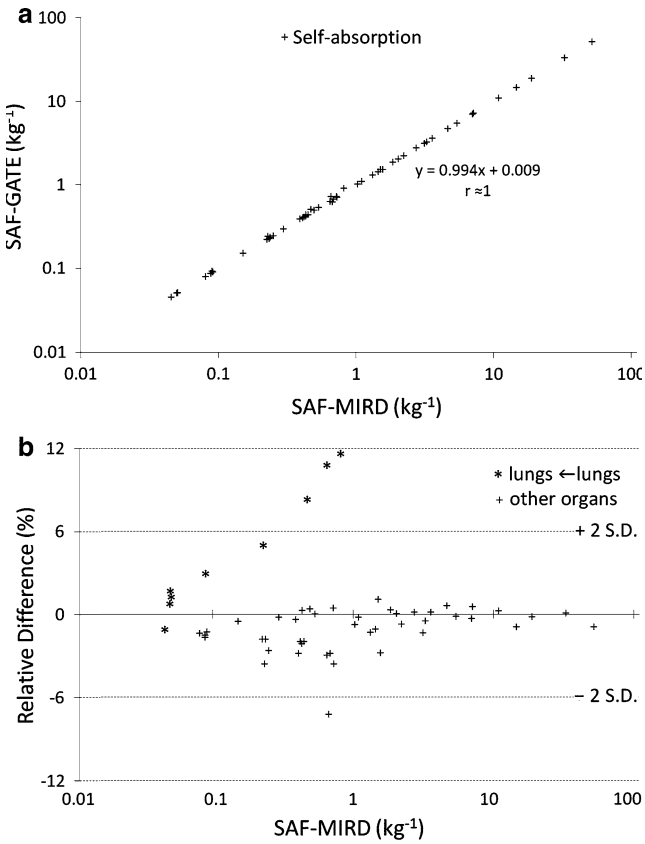

Fig. 1 Comparison of GATE and corresponding MIRD SAF values for self-irradiated organs; **a** scatter plot of two series of data and **b** Bland–Altman analysis for relative differences (RD %) between GATE and MIRD; *SD* standard deviation

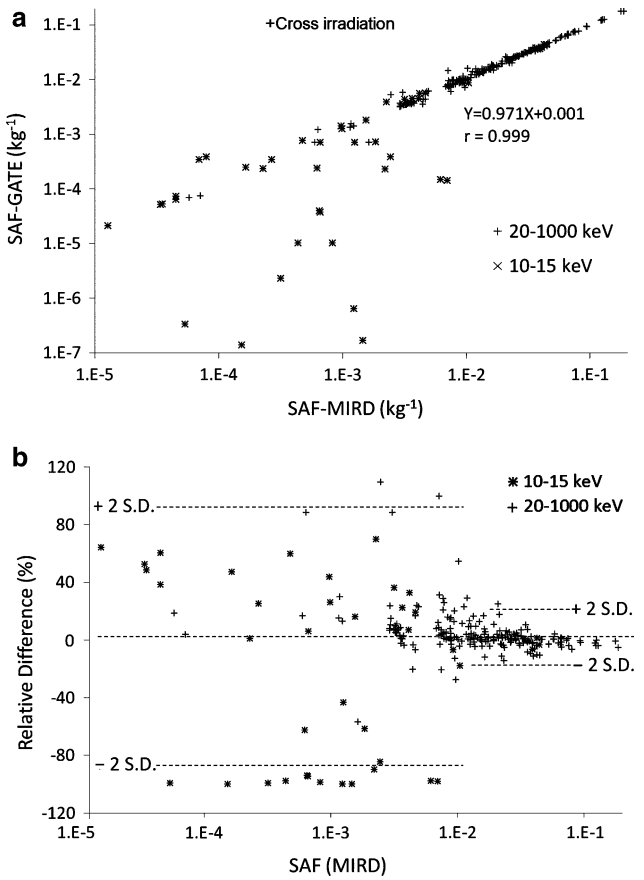

Fig. 2 Comparison of GATE and corresponding MIRD SAF values for cross-irradiated organs; **a** scatter plot of two series of data and **b** Bland–Altman analysis for relative differences (RD%) between GATE and MIRD; *SD* standard deviation

and the cross-irradiation data. The graph shows that for self-absorption, at all photon energies, the relative differences between the GATE/GEANT and the MIRD data are below 3%. For the cross-irradiation data, however, the relative differences were 6–10% at photon energies of 50–1,000 keV and up to 25% at photon energies of 10–30 keV. The SAF values for *adrenals* ←*kidneys*, *adrenals* ←*pancreas,* and against photon energy are shown in Fig. 3b. As can be seen, the SAF values for cross-irradiation increase rapidly from 10 to 50 keV and decrease gradually afterward. At low energies, the photoelectric interaction is predominant while by increasing the photon energy, the Compton interaction gradually becomes predominant. Fig. 3b is representative for all the cross-section data.

Discussion

SAFs for self-absorption

The SAF values derived from the voxelized Snyder phantom show a high correlation with the corresponding MIRD data. The bias between the two series of data is small (−0.16%) and the relative differences are below 5% for the majority of the data points. An exception is the self-absorption of the lungs at photon energies of 10, 15, and 20 keV, where the relative differences are 11.6, 10.7, and 8.3%, respectively. This difference (in self-absorption of the lungs) cannot be related to the Monte Carlo codes or the cross-section tables used to calculate the data. The same difference would have been observed in all organs otherwise. A simple explanation for this observation could be a higher total cross-section and/or density attributed to the lung tissue in our study compared to the MIRD calculations. The inverse dependence of the relative differences on the photon energy supports this explanation. However, the density and the average cross-section of the lungs were set based on the MIRD publication (Snyder et al. 1969). The observed difference in self-absorption of the lungs may partially be related to the method of calculation and the cross-irradiation of the left and right lungs. We performed a single simulation (assuming activity in both lobes of the lungs) to calculate the SAF, as is implied in the SAF definition. Performing two independent

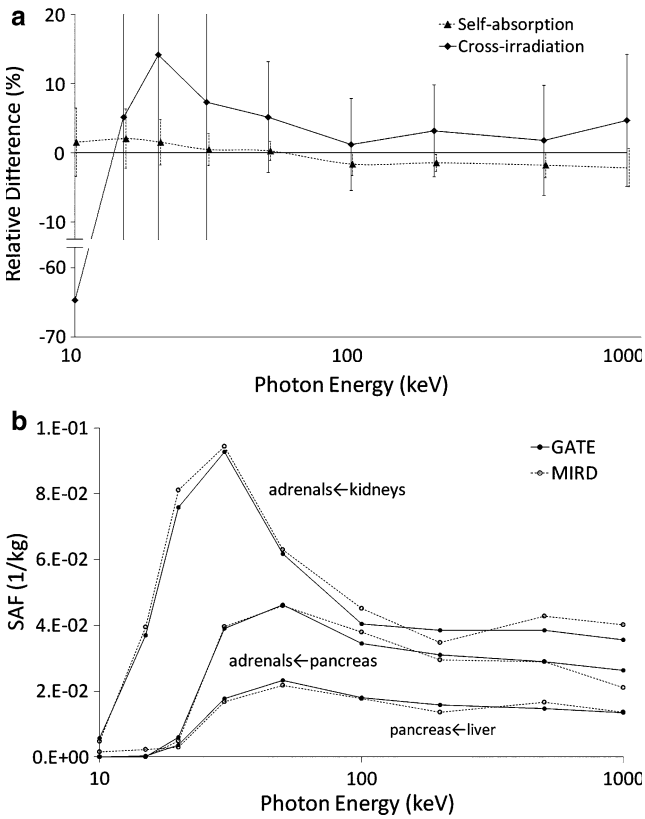

Fig. 3 **a** Average of relative differences between GATE and MIRD plotted against photon energy. The averages were calculated pooling all the data of a given photon energy. **b** SAF values for sampled source-target organs against photon energy. The standard deviation of the data was too small to be shown in the figure

simulations for the left and right lungs would result in a smaller SAF value. When two lobes are considered together, the cross-firing of the left and right lobes are included in the self-absorption of the lungs. This is in agreement with the early acknowledged fact that the absorbed fraction increases with organ mass (Poston 1976). When increasing the mass, less photons can escape from the source organs and, therefore, self-absorption increases. The two lobes of the lung are very close in the Snyder phantom, and there is mainly air in between. In contrast, in our simulation, the two lobes of the lung were considered together like a single big organ. To avoid this error, simulations should be performed independently for each lobe. For other paired organs (kidney, adrenals) that are smaller and far-off, the difference is much less. It is not clear whether this error was considered in the MIRD calculations, though this cannot fully explain the observed differences.

Whatever is the reason behind this observation, the self-absorption data derived from the GATE/GEANT are in good agreement, and there is a high correlation with the corresponding MIRD data where the photon energies were 50–1,000 keV. However, for energy of 10–30 keV, the agreement was questionable.

SAFs for cross-irradiation

There is a good correlation between the GATE/GEANT data and the corresponding MIRD data for cross-irradiation when the photon energies were 50–1,000 keV. However, the correlation is low for 10–30 keV. In some studies, differences between the MIRD SAF values and the corresponding calculated values for low-energy photons have been reported (Larsson et al. 2005; Ferrari and Gualdrini 2007; Kolbert et al. 1997; Zankl et al. 2003). However, none of them used the MIRD phantom; therefore the reported differences may also be due to geometrical differences.

Although the relative difference between our data and the MIRD data is low for high-energy photons (50–1,000 keV) and high for low-energy photons (10–30 keV), this does not imply any direct dependence of the relative difference on photon energy. Fig. 3a reveals only a weak dependence on photon energy in the self-absorption and cross-irradiation data; in contrast, Fig. 2a shows a strong dependence on the absolute values of SAF.

When the photon energy is low, most of the photons are absorbed in the source organ and only a small number of photons penetrate to the target organs. That is, a small fraction of the total energy released is absorbed by the target organs; hence the corresponding SAF values are small. From the statistical point of view, smaller values show a higher statistical uncertainty (random error). Therefore, the poor agreement between the GATE/GEANT and MIRD data for low-energy photons is partly due to poor statistics in the corresponding SAF values. Figure 2b shows that the relative difference significantly depends on the absolute value of the SAF. Inspecting Fig. 3b provides some insight on the random variation in the two series of data. The figure reveals a considerably higher variation in the MIRD data compared to the GATE/GEANT data. The maximum coefficient of variation in our data is 20% (for the smallest SAF value), while in the case of the MIRD data, the coefficient of variation is up to 50% (Snyder et al. 1969).

In the GATE/GEANT code, required cross-sections are derived using the EPDL97, EEDL, and EADL libraries for photons, electrons, and atoms, respectively (Jan et al. 2008). The MIRD data were calculated using a Monte Carlo method in which the cross-sections were derived from McMaster Tables and the ENDL library (McMaster et al. 1969; Plechaty and Terrall 1968; Snyder et al. 1969). Figure 3a reveals that for photons of 50–1,000 keV, there is a small bias ($\approx$2%) between the GATE/GEANT and MIRD data. For self-absorption, the bias is negative (smaller values for GATE/GEANT) while for cross-section the bias is positive. For lower energy photons (10–30 keV), the bias is higher and in reverse direction. This may be

considered as systematic error and a reflection of differences in the cross-section tables used in the MIRD and GATE/GEANT codes. However, this is very difficult to be verified, due to the large number of interactions involved (Salvat et al. 1999). For photons of 50–1,000 keV, different types of interactions in multiple stages are possible. The absorbed energy therefore depends on a random combination of cross-sections that may cancel out point-by-point differences. However, for low-energy photons (10–30 keV), where the photoelectric interaction is predominant and the average number of interactions along the particle track is small, the difference in the cross-sections becomes evident. This may be one reason for the larger difference between the present GATE/GEANT and the MIRD data, for low-energy photons.

Conclusion

In the present study, the SAF values derived from GATE/GEANT and the corresponding MIRD published data were compared. The agreement between the GATE/GEANT results and the MIRD data was found to depend on the absolute values of SAF. On average, the SAF values derived with GATE/GEANT showed an acceptable correlation and agreement with the MIRD data for the photon energies of 50–1,000 keV. However, there was a small bias that may be considered as reflecting differences between the tables of cross-sections used in GATE/GEANT and MIRD. For photons of 10–30 keV, where the absolute values of SAF are small and uncertainties high, there was only poor agreement between the GATE/GEANT results and MIRD data. To some extent, this low agreement was due to differences in cross-section tables used in GATE/GEANT and MIRD. In general, the agreement was acceptable and the results can be considered as validation of GEANT/GATE against MIRD; however, some issues require further investigation.

Acknowledgments This work was supported by a grant funded by the Tarbiat Modares University.

References

Akabani G, Hawkins WG, Eckblade MB, Leichner PK (1997) Patient-specific dosimetry using quantitative spect imaging and three-dimensional discrete fourier transform convolution. J Nucl Med 38(2):308–314

Blaickner M, Kindl P (2008) Diversification of existing reference phantoms in nuclear medicine: calculation of specific absorbed fractions for 21 mathematical phantoms and validation through dose estimates resulting from the administration of 18f-fdg. Cancer Biother Radiopharm 23(6):767–782

Bland JM, Altman DG (2010) Statistical methods for assessing agreement between two methods of clinical measurement. Int J Nurs Stud 47(8):931–936

Bolch W, Lee C, Wayson M, Johnson P (2010) Hybrid computational phantoms for medical dose reconstruction. Radiat Environ Bioph 49(2):155–168

Bouchet LG, Bolch WE, Weber DA, Atkins HL, Poston JWS (1999) Mird pamphlet no. 15: radionuclide s values in a revised dosimetric model of the adult head and brain. Medical internal radiation dose. J Nucl Med 40(3):62S–101S

Bouchet LG, Bolch WE, Blanco HP, Wessels BW, Siegel JA, Rajon DA, Clairand I, Sgouros G (2003) Mird pamphlet no. 19: absorbed fractions and radionuclide s values for six age-dependent multiregion models of the kidney. J Nucl Med 44(7):1113–1147

Caon M (2004) Voxel-based computational models of real human anatomy: a review. Radiat Environ Bioph 42(4):229–235

Chao T-C, Xu XG (2004) S-values calculated from a tomographic head/brain model for brain imaging. Phys Med Biol 49(21):4971–4984

Chiavassa S, Manuel B, Françoise G-V, Damien B, Jean-Rene J, Didier F, Isabelle A-L (2005) Oedipe: a personalized dosimetric tool associating voxel-based models with mcnpx. Cancer Biother Radiopharm 20(3):325–332

Dewaraja K, Wilderman SJ, Ljungberg M, Kora KF, Zasadny K, Kaminiski MS (2005) Accurate dosimetry in ^{131}I radionuclide therapy using patient-specific 3-dimensional methods for spect reconstruction and absorbed dose calculation. J Nucl Med 46(5):840–849

Ferrari P, Gualdrini G (2007) Mcnpx internal dosimetry studies based on the norman-05 voxel model. Radiat Prot Dosim 127(1–4):209–213

Franquiz JM, Chigurupati S, Kandagatla K (2003) Beta voxel s values for internal emitter dosimetry. Med Phys 30(6):1030–1032

Furhang EE, Chui C-S, Sgouros G (1996) A monte carlo approach to patient-specific dosimetry. Med Phys 23(9):1523–1529

Furhang EE, Chui CS, Kolbert KS, Larson SM, Sgouros G (1997) Implementation of a monte carlo dosimetry method for patient-specific internal emitter therapy. Med Phys 24(7):1163–1172

Hadid L, Desbree A, Schlattl H, Franck D, Blanchardon E, Zankl M (2010) Application of the icrp/icru reference computational phantoms to internal dosimetry: calculation of specific absorbed fractions of energy for photons and electrons. Phys Med Biol 55(13):3631–3641

Howell RW, Wessels BW, Loevinger R, Watson EE, Bolch WE, Brill AB, Charkes ND, Fisher DR, Hays MT, Robertson JS, Siegel JA, Thomas SR (1999) The mird perspective 1999. Medical internal radiation dose committee. J Nucl Med 40(1):3S–10S

Jan S, Santin G, Strul D, Staelens S, Assie K, Autret D, Barbier R, Bardies M, Bloomfield P, Brasse D, Avner S, Breton V, Bruyndonckx P, Buvat I, Chatziioannou AF, Choi Y, Comtat C, Donnarieix D, Ferrer L, Glick SJ, Chung YH, Guez D, Honore P-F, Kerhoas-Cavata S, Groiselle CJ, Kohli V, Koole M, Mkrieguer Laan DJD, Kirov AS, Largeron G, Lartizien C, Lazaro D, Maas MC, Lamare F, Mayet F, Melot F, Merheb C, Pennacchio E, Perez J, Maigne L, Rannou FR, Schaart MRDR, Schmidtlein CR, Pietrzyk U, Simon L, Song TY, Vieira J-M, Visvikis D, Walle RVD, Ewieers Morel C (2004) Gate:a simulation toolkit for pet and spect. Phys Med Biol 49(19):4543–4561

Jan S, Santin G, Strul D, Staelens S, Assié K, Autret D, Avner S, Barbier R, Bardiès M, Bloomfield P M, Brasse D, Breton V, Bruyndonckx P, Buvat I, Chatziioannou A F, Choi Y, Chung Y H, Comtat C, Donnarieix D, Ferrer L, Glick SJ, Groiselle CJ, Guez D, Honore P-F, Kerhoas-Cavata S, Kirov AS, Kohli V, Koole M, Krieguer M, Laan DJVD, Lamare F, Largeron G, Lartizien C, Lazaro D, Maas MC, Maigne L, Mayet F, Melot F, Merheb C, Pennacchio E, Perez J, Pietrzyk U, Rannou FR, Rey M, Schaart DR, Schmidtlein CR, Simon L, Song TY, Vieira J-M,

Visvikis D, Walle RVD, Wieërs E, Morel C (2008). Gate4.0.0 users guide. *OpenGATE Collaboration*

Kolbert KS, Sgouros G, Scott AM, Bronstein JE, Malane RA, Zhang J, Kalaigian H, Mcnamara S, Schwartz L, Larson SM (1997) Implementation and evaluation of patient-specific three-dimensional internal dosimetry. J Nucl Med 38(2):301–308

Larsson E, Jönsson B-A, Jönsson L, Ljungberg M, Strand S-E (2005) Dosimetry calculations on a tissue level by using the mcnp4c2 monte carlo code. Cancer Biother Radiopharm 20(1):85–91

Ljungberg M, Sjogreen K, Liu X, Frey E, Dewaraja Y, Strand S-E (2002) A 3-dimensional absorbed dose calculation method based on quantitative spect for radionuclide therapy: evaluation for (131)i using monte carlo simulation. J Nucl Med 43(8):1101–1109

Ludovic F, Nicolas C, Abdalkader B, Albert L, Manuel B (2007) Implementing dosimetry in gate: dose-point kernel validation with Geant4 4.8.1. Cancer Biother Radiopharm 22(1):125–129

Lyra M, Phinou P (2000) Internal doslmetry in nuclear medicine: a summary of its development, applications and current limitations. RSO Magazine 5(2):17–30

Mcmaster WH, Del Grande NK, Mallett JH, Hubbell JH (1969) Compilation of x-ray cross sections, Ucrl-50174, sec ii, rev i, University of California. Livermore, Lawrence Radiation Laboratory, 261 p

Plechaty EF, Terrall JR (1968) An integrated system for production of neutronics and photonics calculational constants. Volume vi. Photon cross sections 1 kev to 100 mev. UNCL. Orig. Receipt Date: 31-DEC-69, Other Information

Poston JW (1976) Effects of body and organ size on absorbed dose: There is no standard patient. *Symposium on radiopharmaceutical dosimetry, Oak Ridge*. TN, USA

Press WH, Teukolsky SA, Vetterling WT, Flannery BP (2007). *Numerical recipes 3rd edn:the art of scientific computing* New York, Cambridge University Press

Saito K, Wittmann A, Koga S, Ida Y, Kamei T, Funabiki J, Zankl M (2001) Construction of a computed tomographic phantom for a japanese male adult and dose calculation system. Radiat Environ Bioph 40(1):69–76

Salvat F, Fernández-Varea JM, Sempau J, Mazurier J (1999) Practical aspects of monte carlo simulation of charged particle transport: mixed algorithms and variance reduction techniques. Radiat Environ Biophys 38(1):15–22

Santin G, Staelens S, Taschereau R, Descourt P, Schmidtlein CR, Simon L, Visvikis D, Jan S, Buvat I (2007) Evolution of the gate project: new results and developments. Nucl Phys B (Proc Suppl) 172:101–103

Sgouros G (2005) Dosimetry of internal emitters. J Nucl Med 46(1):18s–27s

Sgouros G, Kolbert KS, Sheikh A, Pentlow KS, Mun EF, Barth A, Robbins RJ, Larson SM (2004) Patient-specific dosimetry for ^{131}i thyroid cancer therapy using 124i pet and 3-dimensional–internal dosimetry (3d–id) software. J Nucl Med 45(8):1366–1372

Siegel JA, Thomas SR, Stubbs JB, Stabin MG, Hays MT, Koral KF, Robertson JS, Howell RW, Wessels BW, Fisher DR, Weber DA, Brill AB (1999) Mird pamphlet no. 16: techniques for quantitative radiopharmaceutical biodistribution data acquisition and analysis for use in human radiation dose estimates. J Nucl Med 40(2):37S–61S

Smith T, Petoussi-Henss N, Zankl M (2000) Comparison of internal radiation doses estimated by mird and voxel techniques for a "family" of phantoms. Eur J Nucl Med Mol Imaging 27(9):1387–1398

Snyder WS, Fisher HL, Ford MR, Warner GG (1969) Estimates of absorbed fractions for monoenergetic photon sources uniformly distributed in various organs of a heterogeneous phantom. J Nucl Med 3(Suppl):7–52

Snyder W, Ford M, Warner G, Watson S (1975) S, absorbed dose per unit cumulated activity for selected radionuclides and organs. Mird pamphlet no. 11. Society of Nuclear Medicine, New York, NY, USA

Stabin MG (1996) Mirdose: personal computer software for internal dose assessment in nuclear medicine. J Nucl Med 37(3):538–546

Stabin MG (2003) Developments in the internal dosimetry of radiopharmaceuticals. Radiat Prot Dosim 105(1–4):575–580

Stabin MG (2008) Update: the case for patient-specific dosimetry in radionuclide therapy. Cancer Biother Radiopharm 23(3):273–284

Stabin MG, Sparks RB, Crowe E (2005) Olinda/exm: the second-generation personal computer software for internal dose assessment in nuclear medicine. J Nucl Med 46(6):1023–1027

Taschereau R, Chatziioannou AF (2005) Fdg-pet image-based dose distribution in a realistic mouse phantom from monte carlo simulations. In: IEEE Nucl Sci Symp (Conf Rec), 23–29 Oct. 2005. 1633–36

Taschereau R, Chatziioannou AF (2007) Monte carlo simulations of absorbed dose in a mouse phantom from 18-fluorine compounds. Med Phys 34(3):1026–1036

Thiam CO, Breton V, Donnarieix D, Habib B, Maigne L (2008) Validation of a dose deposited by low-energy photons using Gate/Geant4. Phys Med Biol 53(11):3035–3039

Visvikis D, Bardies M, Chiavassa S, Danford C, Kirov A, Lamare F, Maigne L, Staelens S, Taschereau R (2006) Use of the gate monte carlo package for dosimetry applications. Nucl Instrum Meth A 569(2):335–340

Wessels BW, Syh JH, Meredith RF (2006) Overview of dosimetry for systemic targeted radionuclide therapy (start). Int J Radiat Oncol Biol Phys 66(2):S39–S45

Williams LE (2003) Therapeutic applications of monte carlo calculations in nuclear medicine. J Nucl Med 44(6):991

Yoriyaz H, Stabin MG, Dos Santos A (2001) Monte carlo mcnp-4b-based absorbed dose distribution estimates for patient-specific dosimetry. J Nucl Med 42(4):662–669

Zankl M, Petoussi-Henss N, Fill U, Regulla D (2003) The application of voxel phantoms to the internal dosimetry of radionuclides. Radiat Prot Dosim 105(1–4):539–548